



ISSN 0975-413X
CODEN (USA): PCHHAX

Der Pharma Chemica, 2016, 8(10):274-286
(<http://derpharmachemica.com/archive.html>)

Copper corrosion inhibition by 2-Thiobenzylbenzothiazole in 2M nitric acid

D. Ehouman¹, J. S. Akpa², P. M. Niamien^{1*}, D. Sissouma² and A. Trokourey¹

¹Laboratoire de Chimie Physique, Université Félix Houphouët Boigny

²Laboratoire de chimie organique structurale, Université Félix Houphouët Boigny, 22BP 582 Abidjan 22

ABSTRACT

2-Thiobenzylbenzothiazole (2TBBT) has been used as corrosion inhibitor for copper corrosion in 2.0 M nitric acid. The studies were conducted, using mass loss and a quantum chemical method based on Density Functional Theory (DFT). The corrosion rate was found to be concentration and temperature dependent. Information on adsorption of the molecule on the copper surface was assessed through isotherms, including Langmuir, Freundlich and Flory Huggins. The best fit was obtained with the modified Langmuir adsorption isotherm. Thermodynamic adsorption functions and activation ones were determined and analysed. They show a spontaneous adsorption and a chemisorption process. Quantum chemical calculations at B3LYP level with 6-31G (d) basis set lead to molecular descriptors such as E_{HOMO} (energy of the highest occupied molecular orbital), E_{LUMO} (energy of the lowest unoccupied molecular orbital), ΔE (energy gap) and μ (dipole moment). The global reactivity descriptors such as χ (electronegativity), η (hardness), S (softness) and ω (electrophilicity index) were derived using Koopman's theorem and analysed. The local reactivity parameters, including Fukui functions $f(\vec{r})$ and local softness $s(\vec{r})$ were determined and discussed. Furthermore, the relative electrophilicity (s_k^+/s_k^-) and relative nucleophilicity (s_k^-/s_k^+) were also determined and analysed. Experimental and theoretical data are in good agreement.

Keywords: nitric acid, copper corrosion inhibition, DFT, global reactivity descriptors, Local reactivity parameters, relative reactivity descriptors.

INTRODUCTION

Evaluation of corrosion inhibitors for metals in acidic media [1, 2] is an important topic for both academic and industrial points of views. Protection of metallic surfaces [3] can be achieved by addition of specific compounds in the concerned media. Nowadays, the development of new corrosion inhibitors [4, 5], which take the environment into account, has received increasing attention. Thus, molecules containing more numbers of heteroatoms [6] are of interest because of their strong chemical activity, low toxicity and environmental friendly characteristics as corrosion inhibitors.

Thiazole derivatives such as 2-Mercaptobenzothiazole [7], 5-phenylazo-2-Thioxo-Thiazolidin-4-one [8], 5-benzylidene-2, 4-dioxotetrahydro-1, 3-Thiazole [9], have been respectively used as corrosion inhibitors of iron, aluminium and copper in different acidic media.

The mechanism of their action can be different, depending on the metal, the medium and the structure of the inhibitor. However, many papers [10-12], state that organic heterocyclic compounds adsorb on the metallic surface, separating the metal from its environment, preventing then its dissolution. Because organic inhibitors act by adsorption on the metal surface, the efficiency of these compounds [13] depends strongly on their ability to form complexes with the metal. Both π electrons and polar groups containing sulphur, oxygen and nitrogen are fundamental characteristics of this type of molecules. The heteroatoms [14] serve as chelation centres for chemical adsorption.

The effects of molecular structure on chemical reactivity [15-18] have been studied extensively, using quantum chemistry methods: these studies relate inhibition efficiency to the molecular properties of the inhibitors. Recently, DFT methods [19, 20] have been used to analyse the characteristics of the inhibitor/surface mechanism and to describe the structural nature of the inhibitor in the corrosion process.

A perusal of the literature shows that there are very few studies on the inhibition of copper corrosion in acidic media by heterocyclic compounds when compared with iron or aluminium. Thus, in the present work, we investigate experimentally and theoretically, the inhibition efficiency of 2-Thiobenzylbenzothiazole against copper corrosion in 2.0 M nitric acid solution, using mass loss technique and DFT studies.

MATERIALS AND METHODS

Copper specimens

The copper specimens were in the form of rod measuring 10 mm in length and 2.2 mm in diameter; they were cut in commercial copper of purity 95%.

The studied molecule

The structure of 2-Thiobenzylbenzothiazole (formula: C₁₄H₁₁NS₂) is given in Fig.1.

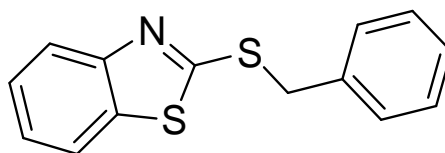


Fig.1: Chemical structure of 2-Thiobenzylbenzothiazole

(2-TBBT) was synthesized in the Laboratory. Its molecular structure was identified by ¹H NMR spectroscopy and mass spectroscopy.

RMN¹H (DMSO-d₆, δ ppm): 2,93 (3H, s, CH₃); 4,6 (2H, s, SCH₂); 7,1-7,5 (9H, m, H_{ar}).SDM: m/e (%) = 65 (15,33); 91 (100%); 224 (27,79); 257 (59,47%).

Solutions

Analytical grade 65% nitric acid solution from Merck was used to prepare the corrosive aqueous solution. The solution was prepared by dilution of the commercial nitric acid solution using double distilled water. The blank was a 2 M HNO₃ solution. Solutions of (2-TBBT) with concentrations in the range of 0.01 mM to 0.5mM were prepared.

Mass loss method

The mass loss method [21, 22] is the most widely used method of inhibition assessment. The simplicity and reliability of the measurement offered by mass loss method [23, 24] is such that the technique forms the baseline method of measurement in many corrosion monitoring programs. The samples were polished successively with fine grade emery papers, cleaned with acetone, washed with double distilled water and dried in moisture free desiccator. Tests were conducted under total immersion conditions of the polished copper specimen in 50 mL of 2.0M nitric acid solutions without and with different concentrations of (2-TBBT). Test solutions were maintained at (308-328K). All tests were made in aerated solutions and were run triplicate to guarantee the reliability of the results. To determine the mass loss at the end of the test, the samples were retrieved from the tests solutions after 1 hour immersion time. The corrosion rate (W) was calculated according to the equation below:

$$W = \frac{m_1 - m_2}{St} \quad (1)$$

Where m_1 and m_2 are respectively the mass (in g) before and after immersion in the test solution, S is the total surface of the sample (in cm²) and t is the immersion time (in h). The inhibition efficiency IE (%) was then calculated using the following relation:

$$IE(\%) = \frac{w_0 - w}{w_0} \times 100 \quad (2)$$

In this equation, w_0 and w are respectively the corrosion rates of copper in the absence and the presence of the tested compounds.

Computational method

To calculate the ground-state energy and the physical properties of (2-TBBT), the Gaussian 03 W package [25] was used. The molecular structure was optimized to a minimum without symmetry restrictions using B3LYP exchange correlation functional, a combination of the Becke three parameter hybrid functional [26] with the correlation functional of Lee, Yang and Parr [27, 28] associated to 6-31 G (d) basis set [29]. Fig. 2 presents the optimized structure of (2-TBBT).

Density functional theory [30] has been proved to be successful in providing theoretical basis for chemical concepts such as electronegativity (χ), hardness (η), softness (S) and local parameters as Fukui function, $f(\vec{r})$ and local softness $s(\vec{r})$.

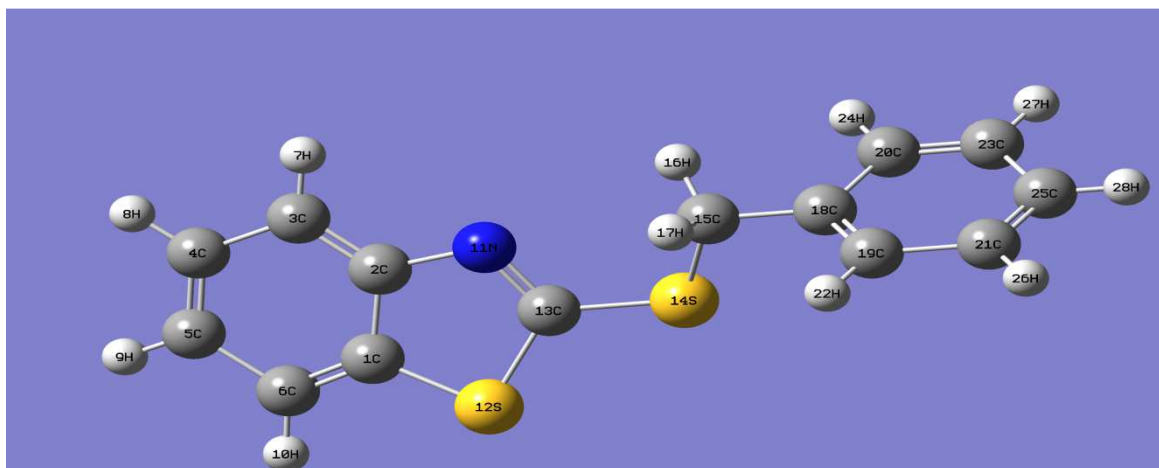


Fig.2: Optimized structure of (2-TBBT) by B3LYP/6-31G (d)

For N-electrons system with total energy E , the electronegativity [31] is given as follows:

$$\chi = -\mu_P = -\left(\frac{\partial E}{\partial N}\right)_{v(\vec{r})} \quad (3)$$

Where μ_P and $v(\vec{r})$ are the chemical and external potentials. The chemical hardness (η) [32] which is defined as the second derivative of E with respect to N is then given by the following relation:

$$\eta = \left(\frac{\partial^2 E}{\partial N^2}\right)_{v(\vec{r})} \quad (4)$$

Softness [33] is the inverse of hardness:

$$S = \frac{1}{\eta} \quad (5)$$

According to Koopmans's theorem [34], HOMO and LUMO energies are related to ionization potential (I) and electron affinity (A) by the following relations:

$$I = -E_{HOMO} \quad (6)$$

$$A = -E_{LUMO} \quad (7)$$

The absolute electronegativity (χ) and the chemical hardness (η) [32] are then written as:

$$\chi = \frac{I+A}{2} \quad (8)$$

$$\eta = \frac{I-A}{2} \quad (9)$$

When two systems, Cu and the inhibitor are brought together, electrons will flow from lower (χ) inhibitor to higher (χ) copper, until the chemical potentials become equal. Therefore the fraction of electrons transferred (ΔN) from the inhibitor molecule to the metal [34] was calculated using the relation below:

$$\Delta N = \frac{\chi_{Cu} - \chi_{inh}}{2(\eta_{Cu} + \eta_{inh})} \quad (10)$$

Where, χ_{Cu} and χ_{inh} denote respectively the absolute electronegativity of copper and that of the inhibitor molecule whereas η_{Cu} and η_{inh} are respectively the absolute hardness of copper and the inhibitor. In our study, we use a

theoretical value of $\chi_{Cu} = 4.98\text{eV/mol}$ [35] and $\eta_{Cu} = 0$ [36] for the computation of the fraction of electrons transferred from the molecule to the metal.

The global electrophilicity, introduced by Parr [37] is given by the relation below:

$$\omega = \frac{\mu_P^2}{2\eta} \quad (11)$$

The local (or site) reactivity (selectivity) of chemical species is represented by local reactivity descriptors. One such descriptor is Fukui function index [38] and is defined as below:

$$f(\vec{r}) = \left(\frac{\partial \rho(\vec{r})}{\partial N} \right)_{v(\vec{r})} = \left(\frac{\partial \mu_P}{\partial v(\vec{r})} \right)_N \quad (12)$$

Where N and $\rho(\vec{r})$ represent respectively, the number of electrons and the electron density at position \vec{r} of the chemical species. After taking care of the discontinuities in $f(\vec{r})$ versus N plot, the “condensed-to -atom” approximations of $f(\vec{r})$, when multiplied by global softness (S) [39] provide local softness values given by:

$$s_k^+(\vec{r}) = [q_k(N+1) - q_k(N)]S = f_k^+ S \quad (13)$$

$$s_k^-(\vec{r}) = [q_k(N) - q_k(N-1)]S = f_k^- S \quad (14)$$

In these equations, $q_k(N)$, $q_k(N+1)$ and $q_k(N-1)$ represent the condensed electronic populations on atom “ k ” for neutral, anionic and cationic systems, respectively. So s_k^+ and s_k^- represent the condensed local softness values of atom “ k ” towards nucleophilic and electrophilic attacks.

To find out the most preferable site (or atom) to be attacked by a nucleophile (or electrophile), two new reactivity descriptors [40] are proposed. These descriptors are defined as follows:

- The relative electrophilicity s_k^+/s_k^- , the highest value of which represents the most preferred atom in a molecule to be attacked by a nucleophile;
- The relative nucleophilicity s_k^-/s_k^+ , the highest value of which represents the most preferred atom in a molecule to be attacked by an electrophile.

The argument in favour of the above proposition is that the individual values s_k^+ and s_k^- are strongly influenced by the basis set and correlation effects. But the ratios of s_k^+ and s_k^- , involving two different electrons densities of systems differing by one in their number of electrons at constant nuclear framework are expected to be less sensitive to the basis set and correlation effects. Several studies [41-44] established the superiority of these newly proposed descriptors over those of s_k^+ and s_k^- .

RESULTS AND DISCUSSION

Mass loss measurements

The corrosion rate curves of copper without and with the addition of (2-TBBT) in 2M HNO_3 at different temperatures are shown in Fig.2. These curves show that corrosion rate of copper in the studied medium, increases with increasing temperature. But this evolution is moderated when the concentration of (2-TBBT) increases.

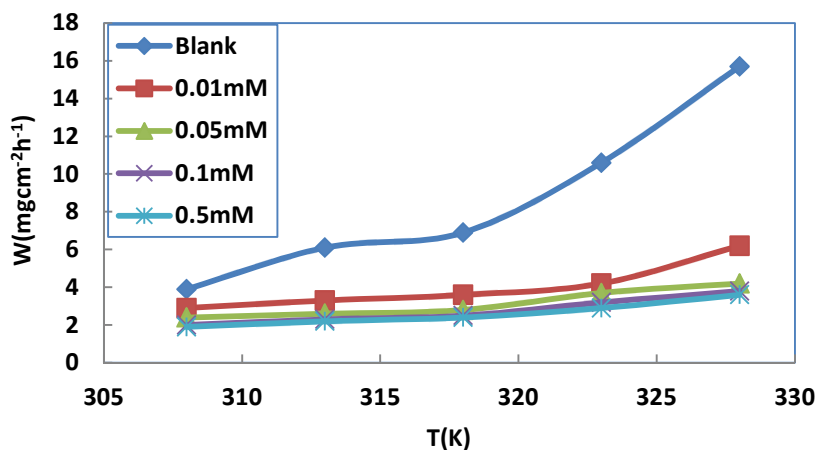


Fig.2: Evolution of corrosion rate with temperature for different concentrations of (2-TBBT)

The inhibition efficiency reaches a value of 77% for the concentration of 0.5 mM (Fig. 3).

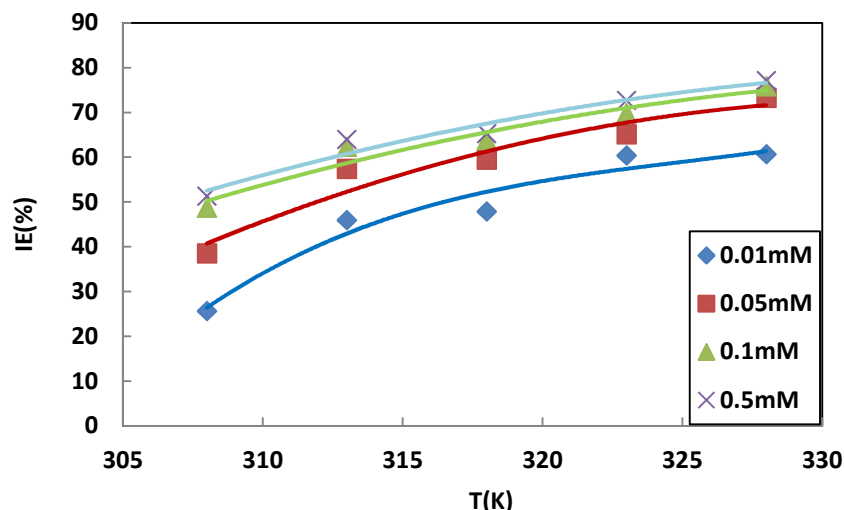


Fig.3: Inhibition efficiency versus temperature for different concentrations of (2-TBBT)

The evolution of the inhibition efficiency for each concentration of (2-TBBT) shows a significant decrease in corrosion rate upon the addition of the investigated molecule to the aggressive solution, revealing the effectiveness of the molecule as a corrosion inhibitor for copper in 2.0 M HNO₃.

A plausible explanation of these results is that the increasing inhibitor's concentration reduces the copper exposed surface to the corrosive environment through the increasing number of adsorbed molecules on its surface which hinders the direct acid attack on the metal surface. The increase of inhibition efficiency with increasing temperature reflects an increase in adsorbed molecules when temperature increases. This behaviour suggests a chemisorption process.

Adsorption isotherms

The adsorption isotherms study gives knowledge about the interaction of inhibitors on the metal surface. The adsorption isotherms tested in this work are the models of Langmuir, Temkin and Flory Huggins. By fitting the rate of surface coverage (θ) and the inhibitor concentration (Fig.4), the best adsorption isotherm obtained graphically is Langmuir adsorption isotherm ($R^2 = 0.999$).

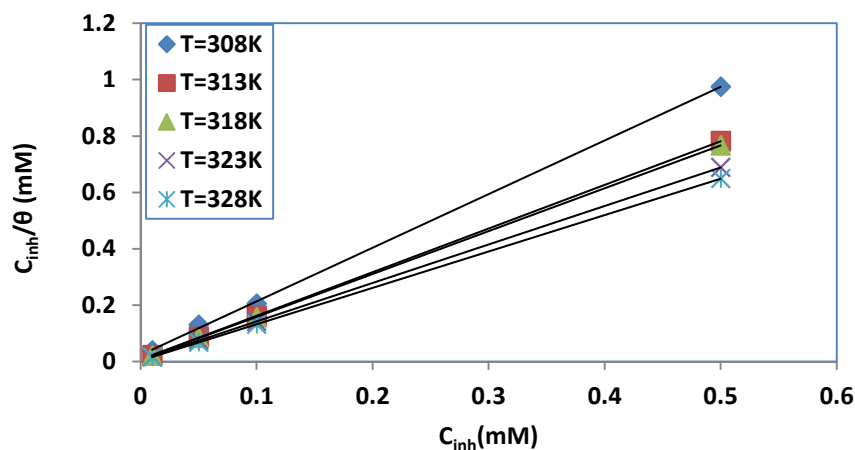


Fig.4: Langmuir adsorption isotherm for (2TBBT) on copper surface in 2M HNO₃

The slopes of the straight lines are different from unity, what suggests [45] interactions between adsorbed species on copper surface as well as changes in the values of Gibbs energy with increasing surface coverage. The results indicate a slight deviation from ideal conditions (all the adsorption sites are equivalent) assumed in the Langmuir adsorption model. Therefore, a modified Langmuir equation [46] must be considered. This equation, which takes into account the deviation from the ideal conditions, may be used as follows:

$$\frac{C_{inh}}{\theta} = \frac{n}{K_{ads}} + nC_{inh} \quad (15)$$

Table 1 gives the obtained Langmuir adsorption parameters for different temperatures.

Table1: Regression parameters of Langmuir isotherm.

T(K)	Correlation coefficient	Slope	Intercept
308	0.999	1.9018	0.0235
313	0.999	1.5493	0.0072
318	0.999	1.5206	0.0062
323	0.999	1.3655	0.0054
328	0.999	1.2907	0.0034

The values of adsorption equilibrium constant K_{ads} were obtained from the intercepts of the straight lines on the C_{inh}/θ -axis. K_{ads} is related [47] to the standard free adsorption energy ΔG_{ads}^0 according to the following equation: $\Delta G_{ads}^0 = -RT \ln(55.5 K_{ads})$ (16) In the above expression 55.5 is the concentration of water in the solution in mol.L⁻¹ [48], R is the perfect gas constant and T is the absolute temperature. The calculated values of ΔG_{ads}^0 are summarized in Table 2.

Table 2: Thermodynamic parameters for the adsorption of (2-TBBT) on copper surface at different temperatures.

T(K)	$K_{ads} (\times 10^3 M^{-1})$	$\Delta G_{ads}^0 (kJ/mol^{-1})$	$\Delta H_{ads}^0 (kJ/mol^{-1})$	$\Delta S_{ads}^0 (J/mol^{-1} K^{-1})$
308	42.5	-27.3	67.3	310
313	138.9	-30.8		
318	161.3	-31.7		
323	169.5	-32.3		
328	294.1	-34.3		

The negative values of ΔG_{ads}^0 [49,50] indicate a spontaneous adsorption of the inhibitor molecule on copper surface while their magnitude suggests a strong interaction between the molecule and metal surface. Generally, the energy values of $-20 kJ mol^{-1}$ or less negative [51] are associated with an electrostatic interaction between charged molecules and charged metal surfaces (physisorption); those of $-40 kJ mol^{-1}$ or more negative [51] involve charge sharing or transfer from the inhibitor molecules to the metal surface to form coordinate bond (chemisorption). In our work the values of ΔG_{ads}^0 range from -34.3 to $-27.3 kJ mol^{-1}$; it can be concluded that the adsorption process is either chemisorption or both physisorption and chemisorption.

The standard adsorption enthalpy (ΔH_{ads}^0) and the standard adsorption entropy (ΔS_{ads}^0) are related by the following equation:

$$\Delta G_{ads}^0 = \Delta H_{ads}^0 - T \Delta S_{ads}^0 \quad (17)$$

So plotting ΔG_{ads}^0 versus T , gives these thermodynamic adsorption parameters: ΔH_{ads}^0 and $(-\Delta S_{ads}^0)$ are respectively the intercept and the slope of the obtained straight line (Fig. 5).

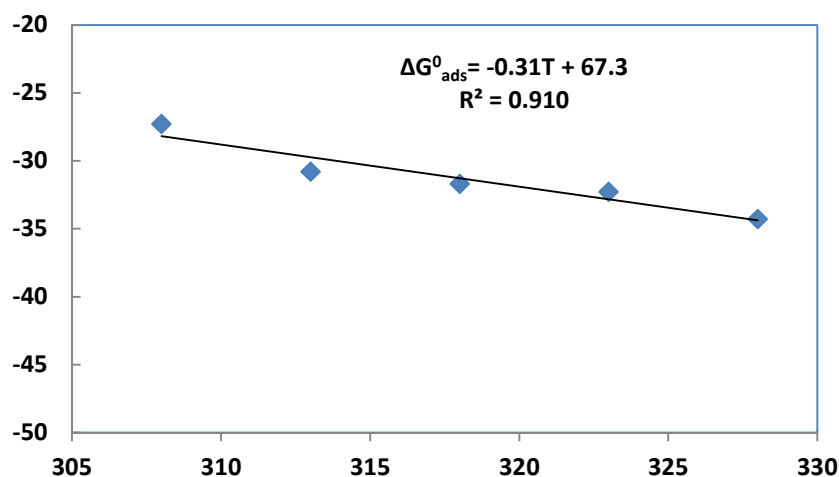


Fig.5: ΔG_{ads}^0 versus T for the adsorption of (2-TBBT) on copper in 2MHNO₃

To distinguish between physisorption and chemisorption, experimental data were fitted to Dubinin-Radushkevich isotherm. This model [52, 53] has been recently used to explain the mechanism of corrosion inhibition onto a metal surface in acidic solution. The model [54] is based on the following equation:

$$\ln\theta = \ln\theta_{max} - a\delta^2 \quad (18)$$

Where θ_{max} is the maximum surface coverage and δ is the Polanyi potential which is given by:

$$\delta = RT \ln \left(1 + \frac{1}{C_{inh}} \right) \quad (19)$$

In this equation, R is the universal gas constant, T is the thermodynamic temperature and C_{inh} is the concentration in $g L^{-1}$ of the inhibitor. Fig. 6 gives the plot of $\ln\theta$ versus δ^2 . The parameters of the model are collected in table 3.

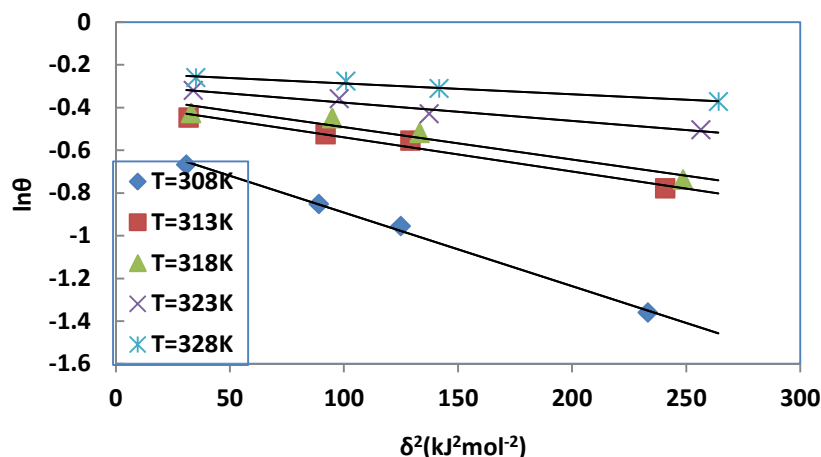


Fig. 6: Dubinin-Radushkevich adsorption model for the adsorption of (2TBBT) on copper

Table 3: Parameters of the Dubinin-Radushkevich isotherm

T(K)	R ²	a (kJ ² mol ⁻²)	E _m (kJ mol ⁻¹)
308	0.997	0.0034	12.13
313	0.976	0.0016	17.68
318	0.943	0.0015	18.26
323	0.965	0.0009	23.57
328	0.979	0.0005	31.62

The values of the constant a are obtained from the slope of the straight lines; this parameter is related to E_m , the adsorption energy which is the transfer energy of 1 mol of adsorbate from infinity (bulk solution) to the surface of the adsorbent. E_m is defined as:

$$E_m = \frac{1}{\sqrt{2a}} \quad (20)$$

The magnitude of E_m gives information about the type of adsorption. E_m values less than 8 kJ mol⁻¹ [54] indicate physical adsorption. In our work E_m values range from 12.13 to 31.62 kJ mol⁻¹, showing a chemisorption process for all the range of temperatures.

Effect of the temperature

Activation parameters are of great importance in the study of the inhibition mechanism of metals. The kinetics functions for the dissolution of copper without and with various concentrations of (2TBBT) are obtained [55] by applying the Arrhenius equation and the transition state equation:

$$\log W = \frac{-E_a}{2.303 RT} + A \quad (21)$$

$$\log \left(\frac{W}{T} \right) = \log \left(\frac{R}{\kappa h} \right) + \frac{\Delta S_a^*}{2.303 R} - \frac{\Delta H_a^*}{2.303 RT} \quad (22)$$

In these equations, E_a is the apparent effective activation energy, R is the molar gas constant and A is the Arrhenius pre-exponential factor; h is the Planck's constant, \aleph is the Avogadro number, ΔS_a^* is the change in activation entropy and ΔH_a^* is the change in activation enthalpy.

Fig.7 and Fig.8 display respectively the plots of $\log W$ and $\log(W/T)$ versus $(1/T)$.

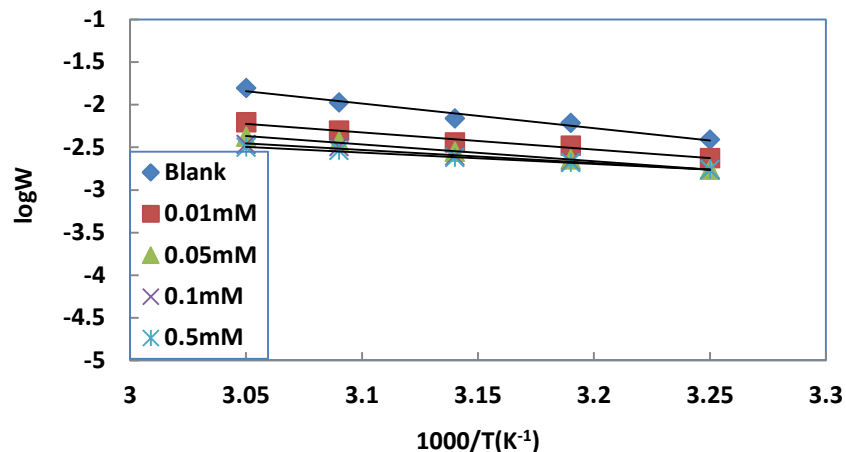


Fig.7: Arrhenius plots for Copper corrosion in 2M HNO₃ solutions without and with (2TBBT)

All graphs show, both in absence and presence of (2TBBT) excellent linearity as expected from equations (21) and (22), respectively. The intercepts of the lines in Fig.7 allow the calculation of the values of the pre-exponential factor (A) and the slopes ($-E_a/2.303R$) lead to the determination of the activation energy (E_a) both in the absence and presence of the inhibitor.

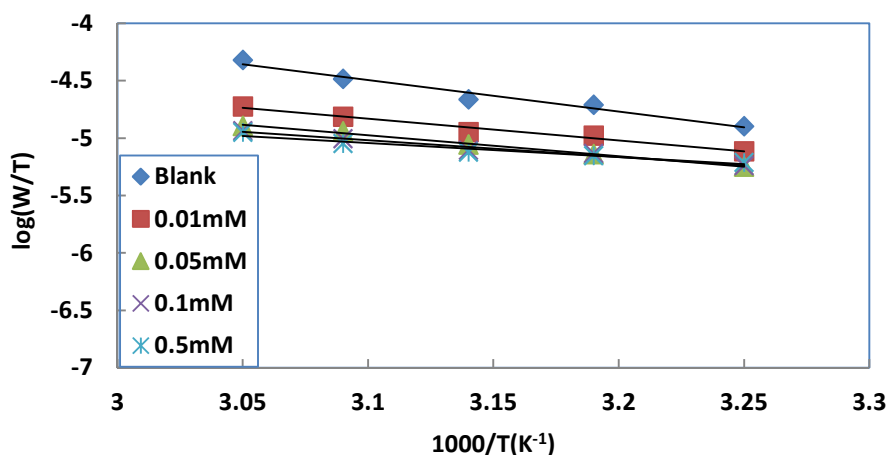


Fig.8: Transition state plots for copper corrosion in 2M HNO₃ with or without (2TBBT)

On the other hand, the obtained straight lines in Fig.8 have a slope of $(-\Delta H_a^*/2.303R)$ and an intercept of $[\log(R/\aleph h) + \Delta S_a^*/2.303R]$. Consequently the values of ΔH_a^* and ΔS_a^* were calculated, respectively. All the results are collected in table 4.

Table 4: Activation parameters for copper corrosion without and with (2TBBT) in 2M HNO₃

	$E_a(kJmol^{-1})$	$\Delta H_a^*(kJmol^{-1})$	$\Delta S_a^*(Jmol^{-1}K^{-1})$
Blank	55.1	52.5	-120.8
0.01mM	38.7	36.2	-177.8
0.05mM	37.8	34.8	-184.7
0.1mM	29.6	28.1	-206.4
0.5mM	25.3	23.6	-220.8

As can be depicted from Table 4, the activation energy in presence of (2TBBT) is lower than that in the blank and E_a decreases with increasing value of the concentration in (2TBBT). This trend in the evolution of the activation energy E_a can be interpreted [56] as an indication for chemical adsorption. The positive sign of change in the

activation enthalpy (ΔH_a^*) obtained in the blank and inhibited solutions reflects the endothermic nature of the dissolution process. The shift towards more negative values of change in activation entropy (ΔS_a^*) with increasing value of the concentration in (2TBBT) imply that the activated complex in the rate determining step represents an association rather than a dissociation, meaning that [57] disordering decreases on going from reactants to the activated complex.

Quantum chemistry studies

Quantum chemical methods [37] have already proven to be very useful in determining the molecular structure as well as elucidating the electronic structure and reactivity. The predicted properties of reasonable accuracy [58, 59] can be obtained from DFT calculations. All the quantum chemical properties are collected in Table 5.

Table 5: Chemical properties of (2TBBT).

Descriptor	Value	Descriptor	Value
E_{HOMO} (eV)	-5.915	χ (eV)	3.374
E_{LUMO} (eV)	-0.833	η (eV)	2.541
ΔE (eV)	5.082	S (eV) ⁻¹	0.393
μ (D)	0.9441	ΔN	0.316
I (eV)	5.915	ω	2.240
A (eV)	0.833	E_N (u a)	-1391.256

According to the frontier molecular orbitals theory of chemical reactivity, electron transition [60] is due to the interaction between the highest occupied molecular orbital (HOMO) and the lowest unoccupied molecular orbital (LUMO) of reacting species. The energy of the highest occupied molecular orbital E_{HOMO} expresses the tendency of a molecule to give electrons to an appropriate acceptor system with a low energy, empty molecular orbital. The lowest unoccupied molecular orbital energy, E_{LUMO} indicates the ability of the molecule to accept electrons. In our work, the higher value of E_{HOMO} (-5.915 eV) and the lower value of E_{LUMO} (-0.833 eV) could explain the good inhibition efficiency of (2TBBT).

The energy gap ($\Delta E = E_{LUMO} - E_{HOMO}$) is an important reactivity parameter. Lower value of this parameter [61] leads to a good inhibition efficiency, because the energy to remove an electron from the last occupied orbital is low. It has been reported [62] that excellent corrosion inhibitors are organic compounds which not only offer electrons to unoccupied orbital of a metal but also accept free electrons from the metal. A molecule with a low energy gap [63] is more polarizable and is generally associated with high chemical reactivity and is considered as a soft molecule. The value of ΔE (5.082 eV) is low compared with that of many molecules in the literature, suggesting good inhibition efficiency.

The dipole moment μ (in Debye) is another important electronic parameter that results from non-uniform distribution of charges on atoms in the molecule. Many authors state that low values of dipole moment [64] favour accumulation of the inhibitor molecules in the surface layer and therefore higher inhibition efficiency. However, many papers indicate that inhibition efficiency increases with increasing values of dipole moment. On the other hand, survey of the literature [67, 68] reveals that several irregularities appeared in case of correlation of dipole moment with inhibitor efficiency. So in general [69], there is no significant relationship between dipole moment values and inhibition efficiencies.

Absolute hardness and softness are important parameters to measure the molecular stability and reactivity of a molecule. The chemical hardness fundamentally represents the resistance

towards the deformation or polarization of the electron cloud of atoms, ions or molecules under small perturbation of chemical reaction. A hard molecule has a large energy gap and a soft molecule has a small energy gap [70]. In our work the studied molecule has a low hardness value (2.541 eV) and a high value of softness (0.393 eV⁻¹) when compared [71, 72] with molecules in the literature.

Generally, the value of ΔN shows inhibition efficiency resulting from electron donation. In our study, $\Delta N < 3.6$: the molecule [73] is donor of electrons and the copper surface is the acceptor. (2TBBT) binds to the copper surface and forms an adsorption layer against corrosion.

Electrophilicity is a property of atoms which signifies the energy lowering process on soaking electrons from donors. The electrophilicity index (ω), measures the stabilization in energy when a system acquires an additional electronic charge from the environment. There is an analogy between electrophilicity and electrical power [74] which has the classical relation ($P = V^2/R$). In this sense the electrophilicity index is a kind of power. Physically, electrophilicity means that it is simultaneously encompasses both the properties of electrophile to acquire an

additional electronic charge driven by μ_p^2 and the resistance of the system to exchange electronic charge with the environment described by η . However, effectively it is conceived as representing the stabilization energy of the system when it becomes saturated by electrons coming from the surroundings. A good, more reactive nucleophile is characterized by lower value of μ_p and ω ; conversely, a good electrophile is characterized by a high value of μ_p and ω .

Fig.9 shows the highest occupy molecular orbital (HOMO) and the lowest unoccupied molecular orbital (LUMO) of (2TBBT).

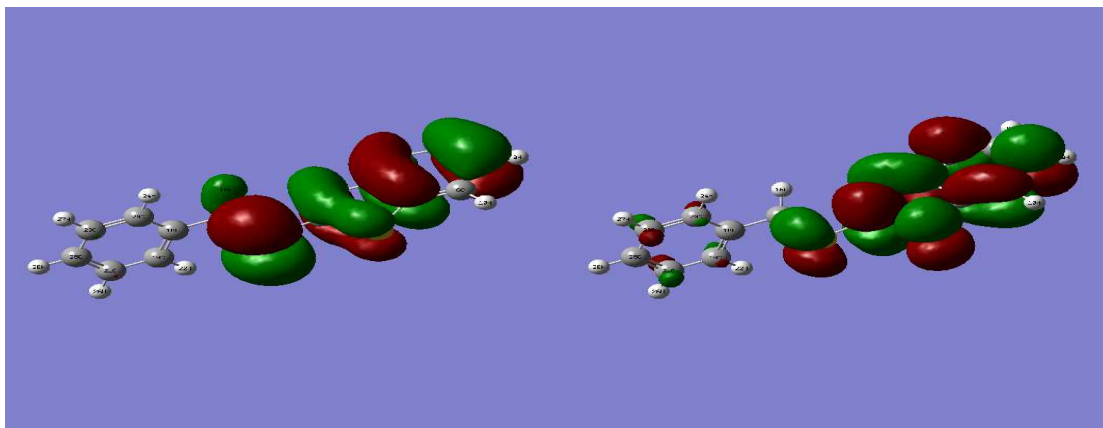


Fig.9: HOMO (left) and LUMO (right) of (2TBBT).

The analysis of Fig.9 shows that the density (HOMO) and (LUMO) for this compound are distributed around the benzothiazole cycles.

Mulliken population analysis [75-78] is used to probe adsorption centres of inhibitors. There is a general consensus by several authors that the more negatively charged an heteroatom is, the more it can be adsorbed on the metal surface through donor-acceptor type reaction [79, 80]. It has also been reported that electrophiles attack molecules at sites of negative charges [81], which means that sites of ionic reactivity can be estimated from atomic charges in a molecules. Thus from the values of Mulliken charges of selected atoms of (2TBBT), listed in Table 7, it is possible to observe that the possible sites for adsorption and reactivity of the studied molecule are C(1), C(3), C(4), C(6), N(11), C(15), C(19), C(20), C(21) et C(23).

Local softness values are computed using equations (13) and (14) where the Fukui functions are identified as:

$$f_k^+ = [q_k(N + 1) - q_k(N)] \quad (23)$$

$$f_k^- = [q_k(N) - q_k(N - 1)] \quad (24)$$

Local reactivity descriptors including Fukui functions, local softness indices and relative electrophilicity and nucleophilicity are collected in table 8.

Table 7: Mulliken atomic charges of some selected atoms of (2TBBT)

Atom	$q_k(N + 1)$	$q_k(N)$	$q_k(N - 1)$
C(1)	-0.094884	-0.137110	-0.113288
C(3)	-0.231941	-0.141874	-0.090067
C(4)	-0.150120	-0.148507	-0.136054
C(6)	-0.231872	-0.176322	-0.165635
N(11)	-0.525675	-0.476235	-0.389880
C(15)	-0.466533	-0.497478	-0.531886
C(19)	-0.179833	-0.162582	-0.159940
C(20)	-0.161297	-0.162557	-0.141342
C(21)	-0.146928	-0.128628	-0.121294
C(23)	-0.138866	-0.128636	-0.117519

Table 8: Fukui functions, local softness indices and relative electrophilicity and nucleophilicity indices for (2TBBT)

Atom	f_k^+	f_k^-	s_k^+	s_k^-	s_k^+/s_k^-	s_k^-/s_k^+
C(1)	0.042627	-0.024223	0.016752	-0.009520	-1.759774	-0.568255
C(3)	-0.090067	-0.013882	-0.035396	-0.005436	6.488042	0.154130
C(4)	-0.001613	-0.012453	-0.000634	-0.004894	0.129527	7.720397
C(6)	-0.055550	-0.010687	-0.021831	-0.004199	5.197904	0.192385
N(11)	-0.049440	-0.086355	-0.019430	-0.033938	0.572520	1.746663
C(15)	0.030945	0.034408	0.012961	0.013522	0.899355	1.111908
C(19)	-0.017251	-0.002642	-0.006780	-0.001038	6.529523	0.153150
C(20)	0.001260	-0.021215	0.000495	-0.008337	-0.059392	-16.83730
C(21)	-0.018300	-0.007334	-0.007192	-0.002882	2.495228	0.400765
C(23)	-0.010230	-0.011117	-0.004020	-0.004369	0.920212	1.086706

The analysis of table 7 shows that according to the Fukui theory of reactivity, C (1) is the nucleophilic attacks centre when C (15) is the electrophilic attacks centre. Nevertheless, regarding the new descriptors, the relative electrophilicity index (s_k^+/s_k^-) and the relative nucleophilicity index (s_k^-/s_k^+), one could design C (4) and C (19) respectively as the preferred electrophilic and nucleophilic attacks sites. To find the effective reactivity centres, we analysed the Mulliken atomic charges; one can see that the atomic charge of C (1) is more positive than that of C (19), what indicates that C (1) should be considered as the preferred nucleophilic attacks site. Moreover, only C(1) is in the LUMO region (lack of electron cloud). For the preferred electrophilic attacks site, we observed that C (15) has the more negative Mulliken atomic charge and is more in the HOMO region (dense electron cloud) than C (4); so it could be considered as the preferred electrophilic attacks site.

CONCLUSION

The following conclusions can be drawn from this study:

1. Inhibition efficiency is temperature and concentration dependent;
2. (2TBBT) adsorbs on copper surface according to modified Langmuir adsorption isotherm;
3. Adsorption thermodynamic functions indicate a spontaneous process and chemisorption;
4. Activation energy and Dubinin Raduskhevich isotherm confirm the chemisorption process;
5. Global reactivity parameters explain the good inhibition efficiency of (2TBBT);
6. Local reactivity parameters and relative nucleophilicity and electrophilicity indices allow determining the probable electrophilic and nucleophilic attacks sites.

Acknowledgements

The authors are grateful to the Central Laboratory of Agrochemical and Ecotoxicology of Abidjan (Côte d'Ivoire) for providing facilities to carry out this work.

REFERENCES

- [1] Ü Ergun, D Yüzer, K C Emregül, *Materials Chemistry and Physics*, **2008**, 109, 492-499.
- [2] S A Umoren, I B Obot, *Surface Review and Letters*, **2008**, 15, 277-286.
- [3] V S Sastri, *Corrosion inhibitors: principles and applications*, New York, John Wiley and Sons Ltd, **1998**, p 237.
- [4] Y Duda, R Govea-Rueda, M Galicia, H I Beltran, L S Zamudlo-Riviera, *JPhys Chem*, **2005**, B 109, 22674-22684.
- [5] L M Rodriguez-Valdez, A Martinez-Villafane, D Glossman-Mitnik, *Journal of Molecular Structure (Theochem)*, **2005**, 713, 65-70.
- [6] F Bentiss, M Traisnel, H Vezin, H F Hildebrand, M Lagrenee, *Corros Sci*, **2004**, 46, 2781-2792.
- [7] M L Zheludkevich, K A Yasakau, SK Poznyck, MGS Ferreira, *Corros Sci*, **2005**, 47, 3368-3383.
- [8] A El-Aziz Fouda, A Al-Sarawy, E El-Katori, *European Journal of Chemistry*, **2010**, 1, 312-318.
- [9] Gy Vastag, E Szöcs, A Shaban, I Bertoti, K Popov-Pergal, E Kalman, *Solid State Ionics*, **2001**, 141, 87-91.
- [10] G Avci, *Mater Chem Phys*, **2008**, 112, 234-238.
- [11] D Gopi, K M Govindaraju, L Kavitha, *Journal of Applied Electrochemistry*, **2010**, 40, 1349-1356.
- [12] M G Sethuraman, P B Raya, *Pigment & Resin Technology*, **2005**, 34, 327-331.
- [13] S K Shukla, M A Quraishi, *Corros Sci*, **2009**, 51, 1007-1011.
- [14] F S de Souza, A Spinelli, *Corros Sci*, **2009**, 51, 642-649.
- [15] Y Karzazi, M El Alaoui Belghiti, A Dafali, B Hammouti, *Journal of Chemical and Pharmaceutical Research*, **2014**, 6, 689-696.
- [16] F Bentiss, M Traisnel, H Vezin, M Lagrenee, *Corros Sci*, **2003**, 45, 371-380.
- [17] P G Abdul-Ahad, SHF Al-Madfai, *Corrosion*, **1989**, 45, 978-980.

- [18] J Cruz, T Pandiyan, E Garcia-Ochoa, *J Electroanal Chem*, **2005**, 583, 8-16.
- [19] L M Rodriguez-Valdez, A Martinez-Villafane, D Glossman-Mitnik, *Journal of Molecular Structure (Theochem)*, **2005**, 716, 61-65.
- [20] N S Patel, P Beranek, M Nebyla, M Pribyl, D Snita, *Int J Electrochem Sci*, **2014**, 9, 3951-3960.
- [21] M Bouklah, B Hammouti, M Lagrenée, F Bentiss, *Corros, Sci*, **2006**, 48, 2831-2842.
- [22] A D Mercer, *Br Corros J*, **1985**, 20, 61-70.
- [23] A R Afidah, J Kassim, *Recent Patents on Mater Sci*, **2008**, 1, 223-231.
- [24] S S Mahmoud, M M Ahmed, R A El-Kasaby, *Advances in Materials and Corrosion*, 1, 36-45.
- [25] M J Frisch, G W Trucks, H B Schlegel, G E Scuseria, M A Robb, J R Cheeseman, J A Montgomery, T Vreven, K N Kudin, J C Burant, J M Millam, S S Iyengar, J J Tomasi, V Barone, B Mennucci, M Cossi, G Scalmani, N N Rega, G A Petersson, H Nakatsuji, M Hada, M Ehara, K Toyota, R Fukuda, J Hasegawa, M Ishida, T Nakajima, Y Honda, O Kitao, H Nakai, M Klene, X Li, J E Knox, H P Hratchian, J B Cross, C Adamo, J Jaramillo, R Gomperts, R E Stratmann, O Yazyev, A J Austin, R Cammi, C Pomelli, J W Ochterski, P Y Ayala, K Morokuma, G A Voth, P Salvador, J J Dannenberg, V G Zakrzewski, S Dapprich, A D Daniels, M C Strain, O Farkas, D K Malick, A D Rabuck, K Raghavachari, J B Foresman, J V Ortiz, Q Cui, A G Baboul, S Clifford, J Cioslowski, B B Stefanov, G Liu, A Liashenko, P Piskorz, I R L Komaromi, M Martin, D J Fox, T Keith, M A Al-Laham, C Y Peng, A Nanayakkara, M Challacombe, P M W Gill, B Johnson, W Chen, M W Wong, C Gonzalez, J A Pople, Gaussian 03, Revision B.05, Gaussian, Inc, Pittsburgh PA, **2003**.
- [26] A D Becke, *J Chem Phys*, **1993**, 98, 5648-5652.
- [27] C Lee, W Yang, R G Parr, *Phys Rev B*, **1988**, 37, 785-789.
- [28] B Miehlich, A Savin, H Stoll, H Preuss, *Chem Phys Lett*, **1989**, 157, 200 -206.
- [29] S G Zhang, W Lei, M Z Xia, F Y Wang, *Journal of Molecular Structure (Theochem)*, **2005**, 732, 173-182.
- [30] R G Parr, W Yang, Oxford University Press: New York, **1989**.
- [31] R G Parr, D A Donnelly, *J Chem Phys*, **1978**, 68, 3801-3807.
- [32] R G Parr, R G Pearson, *J Am Chem Soc*, **1983**, 105, 7512-7516.
- [33] M Berkowitz, S K Ghosh, R G Parr, *J Am Chem Soc*, **1985**, 107, 6811-6814.
- [34] R G Pearson, *Inorg Chem*, **1988**, 27, 734-740.
- [35] R G Pearson, *Proc Natl Acad Sci USA*, **1986**, 83, 8440-8441.
- [36] V S Sastri, J R Perumareddi, *Corrosion*, **1997**, 53, 617-622.
- [37] R G Parr, L Von Szentpaly, S Liu, *J Am Chem Soc*, **1999**, 121, 1922-1924.
- [38] R G Parr, W Yang, *J Am Chem Soc*, **1984**, 106, 4049-4050.
- [39] W Yang, W J Mortier, *J Am Chem Soc*, **1986**, 108, 5708-5711.
- [40] R K Roy, S Krishnamurti, P Geerlings, S Pal, *J Phys Chem A*, **1998**, 102, 3746-3755.
- [41] R K Roy, *J Phys Chem A* **2004**, 108, 4934-4939.
- [42] R K Roy, S Pal, K Hirao, *J Chem Phys*, **1999**, 110, 8236-8245.
- [43] R K Roy, K Hirao, S Pal, *J Chem Phys*, **2000**, 113, 1372-1379.
- [44] R K Roy, N Tajima, K Hirao, *J Phys Chem A*, **2001**, 105, 2117-2124.
- [45] E A Essien, S A Umoren, E E Essien, A P Udoh, *J Mater Environ Sci*, **2012**, 3, 477-484.
- [46] R F Villamil, P Corio, J C Rubin, S S L Agostinho, *J Electroanal Chem*, **1999**, 472, 112-119.
- [47] E Khamis, *Corrosion*, **1990**, 46, 476-484.
- [48] A El Awady, A Abd El Naby, S Aziz, *J Electrochem Soc*, **1992**, 139, 2149-2154.
- [49] E Cano, J L Polo, A La Iglesia, *Adsorption* **2004**, 10, 219-225.
- [50] G Moretti, F Guidi, G Grion, *Corros Sci*, **2004**, 46, 387-403.
- [51] S A Ali, A M El-Shareef, R F Al-Ghamdi, M T Saeed, *Corros Sci*, **2005**, 47, 2659-2678.
- [52] A H Gemeay, A S El-Sherbiny, A B Zaki, *J Colloid Interface Sci*, **2002**, 245, 116-125.
- [53] I D Mall, V C Srivastana, N K Agarwal, I M Mishra, *Colloids Surf A: physicochem Eng Asp*, **2005**, 264, 17-28.
- [54] E A Noor, *J Appl, Electrochem*, **2009**, 39, 1465-1475.
- [55] X Li, S Deng, H Fu, G Mu, *Corros Sci*, **2008**, 50, 2635-2645.
- [56] A K Singh, M A Quraishi, *Mater Chem Phys*, **2010**, 123, 666-677.
- [57] J O M Bockris, A K N Reddy, *Modern Electrochemistry vol 2* Plenum Press, New York, **1977**, p 1267.
- [58] E Kraka, D Cremer, *J Am Chem Soc*, **2000**, 122, 8245-8264.
- [59] C Adamo, V Barone, *Chem Phys Lett*, **2000**, 330, 152-160.
- [60] A Y Musa, A H Kadhun, A B Mohamad, A B Rohoma, H Mesmari, *J Mol Struct*, **2010**, 961, 233-237.
- [61] B Gomez, N V Likhanova, M A Dominguez-Aguilar, R Vela, A Martinez-Palou, J Gasquez, *J Phys Chem*, **2006**, B 110, 8928-8934.
- [62] I Fleming, *Frontier Orbitals and Organic Chemical Reactions*, John Wiley and Sons, New York, **1976**.
- [63] I B Obot, N O Obi-Egbedi, S A Umoren, *Int J Electrochem Sci*, **2009**, 4, 863-877.
- [64] N Khalil, *Electrochimica Acta*, **2003**, 48, 2635-2640.
- [65] M Lagrenée, B Mernari, N, Chaibi, M Traisnel, H Vezin, F Bentiss, *Corros. Sci.*, **2001**, 43, 951-962.

- [66] M A Quraishi, R Sardar, *Journal of Applied Electrochemistry*, **2003**, 33, 1163-1168.
- [67] K F Khaled, K Babic-Samardziza, N Hackerman, *Electrochimica Acta*, **2005**, 50, 2515-2520.
- [68] G Bereket, E Hur, C Ogretir, *Journal of Molecular Structure (Theochem)*, **2002**, 578, 79-88.
- [69] G Gece, *Corros Sci*, **2008**, 50, 2981-2992.
- [70] G Gece, S Bilgic, *Corros Sci*, **2009**, 51, 1876-1878.
- [71] P Udhayakala, T V Rajendiran, S Gunasekaran, *Journal of computational Methods in Molecular Design*, **2012**, 2, 1-15.
- [72] P Udhayakala, T V Rajendiran, *Der Pharma Chemica*, **2015**, 7, 92-99.
- [73] I Lukovits, E Kalman, F Zucchi, *Corrosion*, **2001**, 57, 3-8.
- [74] P Chaquin, *Chem Phys Lett*, **2008**, 458, 231-234.
- [75] F H Assaf, M Abou-Krish, A S El-Shahawy, M Makhoul, H Soudy, *Int J Electrochem Sci*, **2007**, 2, 169-181.
- [76] J Fang, J Li, *Journal of Molecular Structure (Theochem)*, **2002**, 593, 179-185.
- [77] R Hasanov, M Sadikoglu, S Bilgic, *Appl Surf Sci*, **2007**, 253, 3913-3921.
- [78] N K Allam, *Appl Surf Sci*, **2007**, 253, 4570-4577.
- [79] M Ozcan, I Dehri, M Erbil, *Appl Surf Sci*, **2004**, 236, 155-164.
- [80] W Li, Q He, C Pei, B Hou, *Electrochim Acta*, **2007**, 52, 6386-6394.
- [81] M Ozcan, I Dehri, *Prog Org Coat*, **2004**, 51, 181-187.